Renewable Energy, Volume 35, January 2010, Pages 1424–1435

Two-sided Wind Catcher Performance Evaluation Using Experimental, Numerical and Analytical Modeling

H. Montazeri*, F. Montazeri, R. Azizian, S. Mostafavi

Department of Mechanical Engineering, School of Engineering, Yazd University, Yazd, Iran

Abstract: Experimental wind tunnel and smoke visualization testing as well as CFD and analytical modeling were conducted to investigate the performance of a two-sided wind catcher. This type of wind catcher is divided internally into two halves for the purposes of air supply and extract. In this study, the two-sided wind catcher model was constructed of two similar one-sided wind catcher models, which were attached together back to back. These one-sided models are 1: 40 scale models of Kharmani's School wind catcher in the city of Yazd. Experimental investigations were carried out using an open-circuit wind tunnel and both the induced volumetric airflow into the building and the pressure coefficients around all surfaces of the wind catcher model were measured at various wind angles. Furthermore, the CFD simulation was also used to evaluate the pressure coefficient distribution and airflow pattern around and through the wind catcher. Additional experimental tests and computational fluid dynamics simulation of the wind catcher in the wind tunnel were also conducted in order to assess the accuracy of measurement procedures and the uncertainty of experimental results. This article also represents a semi-empirical approach in which experimental data were used for a detailed analytic model, in order to provide an accurate estimate of the performance of wind catchers. It was found that for an isolated two-sided wind catcher model, the maximum efficiency is achieved at the angle of 90 degrees. At this air incident angle the wind catcher efficiency increases approximately 20% more than the one at zero angle. The experimental investigations demonstrated the potential of two-sided wind catcher for enhancing the natural ventilation inside buildings. It can be seen CFD simulation and analytical modeling results have a good agreement with the experimental results. Theoretical modeling can also help to assess the accuracy of measurement procedures and the uncertainty of experimental results.

Keywords: Two-sided wind catcher, Natural ventilation, Experiment, wind tunnel, CFD, Analytical model, Flow visualization

1. Introduction

Natural ventilation has become an increasingly attractive method for reducing energy consumption and cost. This environmental friendly technology also helps to provide acceptable indoor environmental quality and maintain a healthy, comfortable, and productive indoor climate rather than the more prevailing approach of using mechanical ventilation.

Wind catchers or Baud-Geers (as they are called in Persian language), have been used over centuries in the hot arid regions of Iran and the countries of the Persian Gulf to provide natural ventilation and passive cooling [1-3]. The wind towers maintain natural ventilation through living spaces due to wind as well as buoyancy effects [4]. The wind catcher system captures wind from external air stream and induces it into the building in order to cool the inside occupant directly by increasing the convective and evaporative heat transfer from the inner part surfaces. It cools the inner part indirectly by removing the stored heat inside the building structure [5].

Wind catcher is normally a tall structure with the height between 5 to 33 m mounted on the roof of a building. The design of these systems has been traditionally based on the personal experience of architects as well as the dignity, wealth and social position of the house owners and differed in the height of tower, cross-section of the air passages, placement and the number of openings as well as placement of the tower with respect

* **Corresponding author:** Hamid Montazeri, Department of Mechanical Engineering, School of Engineering, Yazd University, Yazd, Iran.
E-mail address: h.montazeri@tue.nl; montazeri_hamid@yahoo.com

to the structure it cools [6]. Figure 1 shows several ancient wind catchers with different configurations in the city of Yazd in Iran.

Karakatsanis et al. [2] determined wind pressure coefficients at various openings of a square wind catcher by testing a scale model of the building in a boundary layer wind tunnel. The tests were conducted on an isolated tower, the tower and the adjoining house, and the tower and the house surrounded by a courtyard. Using measured pressure coefficients natural ventilation through the building was estimated analytically. Elmualim and Awbi [7] carried out experimental investigations and computational fluid dynamics (CFD) simulations to evaluate the performance of square and circular section wind catchers. The achieved results showed that the efficiency of the four-sided wind catcher is much higher than that of the circular one for the same wind speed. They claimed these results had arisen from the fact that the sharp edges of the square wind catcher create a large region of flow separation and a higher pressure difference across the device. Montazeri and azizian [5] evaluated the performance of a one-sided wind catcher using experimental wind tunnel and smoke visualization testing. The induced air flow rate into the test room and the pressure coefficients around all surfaces of its channel were measured for different values of approaching air incident angles. Neglecting the dependence of discharge coefficient on the flow direction, natural ventilation performance of one-sided wind catcher was estimated using a non-dimensional analytical model. Li and Mak [8] used CFD technique to examine the performance of a 500 mm square section wind catcher which demonstrated good agreement with Elmulaim and Awbi's [7] data, although this is limited to overall ventilation rates. Elmualim [9] studied a similar wind catcher device, including dampers, diffuser, and a heat source to assess the ventilation capabilities of the device. The results yielded a good correlation between the numerical simulation and experimental measurements. Hughes and Ghani [10] used CFD to calculate net flow rates through a 1000 mm square wind catcher. They concluded that the CFD results show good correlation, and the grid adaption technique is a well-recognised practice for achieving reliable results.

Several academic studies have been reported in the field of natural ventilation in which flow rate is estimated using simple envelope flow models [2, 5, 11-15]. In these models it is normally assumed that losses which occurred as the air passes through an opening can be modeled using an equivalent coefficient of discharge. In these cases values similar to those measured for orifice plates are commonly used [2, 11-14].

This work focuses on studying the hydrodynamic behavior of a two-sided wind catcher. This kind of wind catcher has two equal halves for the purposes of air supply and extract. In the present study a scale model of a two-sided wind catcher was employed in a wind tunnel and the induced airflow rate into the test room and the pressure coefficients around all surfaces of the wind catcher model were measured accurately for different values of approaching air incident angles. Furthermore the CFD commercial code was also used to evaluate the pressure coefficient distributions and airflow pattern around and through the wind catcher. Additional experimental tests and CFD simulation in the wind catcher were also conducted in order to assess the accuracy of measurement procedures and the uncertainty of experimental results. Also using measured pressure coefficients the theoretical values of ventilated air flow were estimated to evaluate ability of simplified models in natural ventilation studies.

2 Wind tunnel experimental set-up and measurement procedures

The experimental investigations were conducted in an open-circuit subsonic wind tunnel located in the thermodynamics laboratory of the School of Mechanical Engineering of Yazd University. This wind tunnel is designed for the experimental testing of natural ventilation devices and has a test section with a height, width, and length of 46, 46, and 360 cm, respectively. According to the dimensions of the model and the wind tunnel cross-section, the scaled model produced a maximum wind tunnel blockage of 5.5 per cent (for a wind angle of 90º), and no corrections were made to the pressure measurements obtained with these configurations.

In aeronautical studies, it is normally required that the Reynolds number for the model and for the full-scale body it represents be the same. This would require that the 1:40 scale model be tested at velocities about 40 times greater that of the prevailing winds, something not possible to accomplish. Nevertheless, it has been found that the hydrodynamic behavior and the pattern of the airflow in buildings are independent of the Reynolds number, which is due to the forced flow separation at the angular corners of these geometries [5].

To recognize the flow pattern in and over the wind catcher model, smoke visualization tests were also carried out. To flow visualization, both roof and one side of a two-sided wind catcher model were built of glass and the model was exposed to a free stream air velocity of 3 m/s to obtain smoke of a sufficiently high concentration. These flow visualization tests helped to identify the supply and extract segments during all tests.

2.1 The wind catcher model

A two-sided wind catcher has two openings and two separated underneath channels and is often employed in areas where there is a prevailing wind. In this study, the two-sided wind catcher model was constructed from two similar one-sided wind catcher models, which were attached together back to back. These one-sided models are

1: 40 scale models of Kharmani's School wind catcher. Figure 2 shows Kharmani's School Baud-Geer and also an ancient two-sided wind catcher.

The two-sided scale model was made of wood and 23 internal pressure taps were installed at three surfaces of each channel in order to measure static pressure at those points. Three surfaces of the windward side (at zero air incident angle) are named S_W(L), S_W(P), and S_W(R), which are the left, projected, and right surfaces, respectively. Likewise, surfaces of the leeward side are named S_L(L), S_L(P), and S_L(R). Several tiny and sensitive pitot and static tubes were used to measure the airflow rate passed through each channel. The results, which were confirmed by smoke visualization tests, indicate that each opening may act as air supply or extract; hence it was required that these pitot and static tubes to be set at both the top and bottom segments of channels.

The model was so constructed that it could be rotated inside the test section in order to provide different approaching air directions. In this study, the wind direction was varied in the range of 0–90◦ with an interval of 15º. The wind catcher model was connected to a house model, which was erected beneath the wind tunnel. The house model had a vertical openable window that was placed at the back of it. Figure 3 shows the constructed model under investigation with the attached pressure taps and pitot and static tubes at the bottom of the windward channel. This figure also shows how the wind catcher model was attached to the house model in the wind tunnel. Figure 4 shows the isometric view of this two-sided wind catcher model and the house model, which is attached to it along with their dimensions.

2.2 Measurements procedures

2.2.1 Pressure coefficients

The external pressure field induced by wind is the most important factor, which influences internal flows in a naturally ventilated structure. In this study, all pressure measurements were referred to the upstream dynamic pressure using the reference velocity in the wind tunnel for the case of uniform wind. The wind pressure coefficient C_P is calculated using the following formula

$$C_P = \frac{p - p_s}{1/2\,\rho V_{ref}^2} \tag{1}$$

where p is the surface pressure that was measured with the use of several pressure taps. These pressure taps were neatly placed at apertures and underneath channels of the model. In this equation, p_s is the upstream static pressure and $1/2\,\rho V_{ref}^2$ is the dynamic pressure of the uniform wind. Upstream static and total pressures were measured using a pitot–static tube that was placed 16.5 *cm* upstream of the test model and 12 *cm* above the wind tunnel floor.

2.2.2 Ventilation airflow

In this study, several pitot and static tubes were used in order to determine the induced airflow rate into the test room. For this purpose, stainless steel tubes were employed, each with an outside diameter of 1.2mm. The probe diameter ratio of these square-ended pitot tubes was equal to 0.8. The results of CFD simulation in this study and the results of other investigations [5, 8] show that at the entrance openings and near the lower edge, there exists a separated flow and a circulation zone due to the rotation of the incoming air stream into the underneath air channel. This causes a non-uniform flow inside of it. Therefore, it was decided to use more pitot tubes at the bottom of the windward channel. Then, in order to measure induced airflow rate, 20 pitot and 11 static tubes were installed at the bottom of the windward channel. The leeward segment for all approaching air incident angles and the windward side for some approaching air incident angles act as suction devices. In these cases, 10 pitot and 5 static tubes were employed at the top of the extract channel to measure the ventilation airflow rate.

The cross-sectional area of this channel was divided into several portions and the airflow rate passed through it was calculated as follows

$$Q = \sum_{i=1}^{n} A_i V_i \tag{2}$$

where Q is the flowrate through the channel of the wind catcher and Ai and Vi are the area and velocity of portion i, respectively.

The calculated airflow rate was strongly dependent on the measured velocities which were determined using pitot and static tubes. The pitot or static probe may experience an incoming flow that is not parallel to its centre-line either because of physical misalignment to the predominant flow direction or of large variations in the angle

of a turbulent or unsteady flow. The directional sensitivity of the probe will depend on the tip shape, the probe diameter ratio d_{in}/d_{out}, and the Mach and Reynolds numbers [17]. For this reason, experimental tests were carried out to determine the yaw characteristics of probes used in this study. Pitot sensitivity was determined using four pitot tubes arranged with different distances from each other. The tests were conducted in the uniform flow wind tunnel for three different wind velocities of 10, 15, and 20 m/s for wind angles of 0 to 45º in increments of 2.5. The angle characteristics of these total-pressure tubes are shown in Fig. 5 for a velocity of 20 m/s. The difference between the probe indication and true total pressure (P_t- $P_{t,\ ind}$) is expressed as a fractional part of the impact pressure (P_t -P_s), and is plotted against flow angle α. The results show that these square-ended probes begin to show error near 18º of flow inclination. These results have good agreement with the experimental results of other researchers [18]. In addition, the same results were obtained for the static tubes used in this experiment.

2. Computational fluid dynamic

CFD analysis is intended to be more beneficial than wind tunnel testing to explore some of the properties of wind catcher systems, e.g. short circuiting, vortex regions, supply and extract segments, and profile of velocity and total pressure. CFD is a reliable tool to evaluate the accuracy of measurement procedures and also to obtain more accurate results.

A commercial CFD package FLUENT has been used in this study to simulate the airflow in and around the two-sided wind catcher connected to the room. The analysis was conducted at steady state and with a three-dimensional model. A quick scheme was used as the finite difference scheme with the SIMPLE pressure–velocity-coupling algorithm. Three different turbulence models were investigated for determining the pressure distribution and airflow around and through the wind catcher. These models are k−e, RNG k−e, and the Reynolds stress model.

2.1 Grid generation

In order to evaluate the hydrodynamic behavior of a two-sided wind catcher a geometrical representation of the wind tunnel testing set-up was produced in the Gambit program. The simulation was carried out in the range of 0-90° with an interval of 15° and for a uniform wind velocity of 20 m/s. For the wind angles of 0° and 90°, calculation area was half the wind tunnel cross section with a symmetry plane and for this case hexahedral grids were used. For other wind angles (15-75°) whole wind tunnel testing set-up was simulated and unstructured grid was used. To investigate the solution independency from the grid many meshes were generated. Figure 6 shows the meshing of the modeled wind catcher along with boundary conditions which used in this investigation. Boundary conditions for numerical simulation of the flow are chosen to be the same as the conditions in the wind tunnel during the experiments. Table 1 shows the summary of CFD prediction.

3. Analytic model

One of the most questionable issues in both simple and detailed ventilation models used to predict passive cooling is related to the attribution of discharge coefficients. In order to improve our knowledge of real values of flow resistance coefficients in buildings, a semi-empirical approach is presented in which for a detailed analytical model the experimental data related to one and two-sided wind catchers are used.

3.1 Flow network analysis

Flow the air through a building with different number of openings can be estimated by replacing the building with its equivalent flow network [13, 16]. The amount of air flowing through an opening j may be expressed by

$$Q_j = \left(P_j - P_i\right) / R_{ij} \tag{3}$$

Where P_i is the air pressure inside the building and R_{ij} is the flow resistance of the opening j which can be stated as follow:

$$R_{ij} = \left[0.5\rho\left(p_j - p_i\right)\right]^{0.5} / A_j C_{d\,j} \tag{4}$$

Here A_j is the area and $C_{d\,j}$ is the discharge coefficient of the opening j. Substituting Eq. (3) into Eq. (4) gives

$$Q_j = A_j C_{dj}\left[\frac{2}{\rho}\left(P_j - P_i\right)\right]^{0.5} \tag{5}$$

Pressure difference mentioned in the previous equation can be expressed using the following statement:

$$p_j - p_i = 0.5\rho V_{ref}^2\left|\left(C_{pj} - C_{pi}\right)\right| \tag{6}$$

Where V_{ref} is the velocity of the uniform wind, C_{pj} is the pressure coefficient at opening j, and C_{pi} is the pressure coefficient inside the room. Substituting Eq. 6 into Eq. 5, leads to

$$Q_j = A_j C_{dj} V_{ref}\left(C_{pj} - C_{pi}\right)\left(\left|C_{pj} - C_{pi}\right|\right)^{-0.5} \tag{7}$$

Considering the Law of Mass Conservation, this equation appears as

$$\sum_{j=1}^{N} A_j C_{dj} V_{ref}\left(C_{pj} - C_{pi}\right)\left(\left|C_{pj} - C_{pi}\right|\right)^{-0.5} = 0 \tag{8}$$

For a building with N openings, Eqs. 7 and 8 form N+1 simultaneous equations which can be easily solved for the unknowns C_{pi} and Q_j.

3.2 Pressure coefficients

In the case of wind-induced ventilation, the knowledge of internal and external pressure coefficient amounts for each opening is required to find out the pressure difference across this opening. These coefficients are usually obtained experimentally or from standard pressure coefficients data.

With the help of the model developed in the previous section, ventilation rates generated by a two-sided wind catcher for known values of C_p and C_d will be computed. The C_p values are related to the design of the wind catcher and depend on wind direction. Here, the C_p values measured in the wind tunnel investigation were used.

The wind tunnel study on natural ventilation performance of a one-sided wind catcher was also carried out by Montazeri and Azizian [5] and both the induced flow rate and Cp were measured at various wind angles. The data measured for one-sided and two-sided wind catchers is represented in Table 2 for different air incident angles.

3.3 Estimation of discharge coefficients

Figure 7 represents related flow network for one-sided and two-sided wind catcher used in this study. The one-sided wind catcher and the attached room can be considered as a channel and as it is shown in Fig. 7-a the air flow rate can be estimated by using Eq. (7)

$$Q = A_o C_{dt} V_{ref}\left(C_{po} - C_{pw}\right)\left(\left|C_{po} - C_{pw}\right|\right)^{-0.5} \tag{9}$$

Where C_{po} and C_{pw} are average pressure coefficients at the opening of the wind catcher and at the window of the house respectively. In this Eq. C_{dt} is defined as total discharge coefficient. C_p and airflow rate values from Table 2 are both used and then Eq. (9) is solved for values of total discharge coefficient. The results are shown in Table 2. It seems that the total discharge coefficient is independent of the air incident angle though there are some fluctuations near the transition angle.

The air flow rate into the one-sided wind catcher can be estimated using flow network model shown in Fig. 7-b, Eqs. (7) and (8)

$$Q_{opening\rightarrow room} = A_o C_{do} V_{ref}\left(C_{po} - C_{pi}\right)\left(\left|C_{po} - C_{pi}\right|\right)^{-0.5} \tag{10-a}$$

$$Q_{room\rightarrow window} = A_w C_{dw} V_{ref}\left(C_{pw} - C_{pi}\right)\left(\left|C_{pw} - C_{pi}\right|\right)^{-0.5} \tag{10-b}$$

$$A_o C_{d\,o} V_{ref} \left(C_{p_o} - C_{p_i}\right) \left|C_{p_o} - C_{p_i}\right|^{-0.5} + A_w C_{d\,w} V_{ref} \left(C_{p_w} - C_{p_i}\right) \left|C_{p_w} - C_{p_i}\right|^{-0.5} = 0 \qquad \text{(10-c)}$$

Eq. (10-c) can be solved for C_{p_i}.

$$C_{p_i} = \frac{C_{d\,o}{}^2 . C_{p_o} + C_{d\,w}{}^2 . C_{p_w}}{C_{d\,o}{}^2 + C_{d\,w}{}^2} \qquad (11)$$

For a one-sided wind catcher system we have $Q_{opening \to window} = Q_{opening \to room} = Q_{room \to window}$. Substituting Eq. (11) into Eq. (10-a) and by combining with Eq. (9), Eq. (12) can be derived as follow

$$C_{d\,t} = \frac{C_{d\,o} . C_{d\,w}}{\left(C_{d\,o}{}^2 + C_{d\,w}{}^2\right)^{0.5}} \qquad (12)$$

With the use of pressure coefficients and air flow rate values from Table 2 are used and with the use of Eq. (12), values for discharge coefficient at openings of the wind catcher and at the window of the house are successively altered until an acceptable agreement between theory and experiment is achieved. Note that in this study it is assumed that the discharge coefficient is independent of wind direction. In this case the value of the discharge coefficient at the window is equal to 0.75, whereas this is 0.4 for windward and leeward openings.

4. Comparison factor

In order to achieve an optimum configuration for wind catcher systems, it is necessary to define a parameter through which the efficiency of wind catchers from economic, designing and ventilated airflow viewpoints will be compared to each other. These parameters appear in a comparison factor that can be defined as follows.

$$\text{Comparison Factor} = \frac{Q^*_{\alpha 1}}{Q^*_{\alpha 2}} \qquad (13)$$

where $Q^*_{\alpha 1}$ and $Q^*_{\alpha 2}$ are the induced airflows per volume unit of one-sided and two-sided wind catchers, respectively. In this study, the two-sided wind catcher was constructed of two similar one-sided wind catchers. Consequently, comparison factor can be stated as follow:

$$\text{Comparison Factor} = \frac{2Q_{\alpha 1}}{Q_{\alpha 2}} \qquad (14)$$

5. Results and Discussions

Table 3 shows a comparison between the measured and calculated airflow rate through windward, leeward, and window of the room for the various turbulence models at air incident angles of 0° and 90°. In general, it shows that good agreement has been achieved. The results show some variations for the various turbulence models. The results of the calculated flow rate show relatively little variation for the RSM and RNG k−e turbulence models compared with the experimental data at zero air incident angle and for both RSM and standard k-e at 90°. Therefore in this study RSM was used for all simulations.

Figure 8 shows the wind tunnel experimental and CFD results of the volumetric airflow through the windward and leeward sides and through the window of the house. In this figure the supply and the extract segments are recognized by positive and negative values of airflow respectively. In the experimental study, the volumetric airflow quantities through the windward and leeward sides of the wind catcher were measured experimentally and the airflow through the window was determined using the algebraic sum of these two values. Air flow patterns using a two-sided wind catcher with respect to the wind directions may be stated in three parts. In the first region, for which the wind angle varies from 0° to 50°, the average pressure coefficient of the windward opening will be larger than that of the window and the leeward side; hence the wind catcher captures wind from an external air stream and induces it into the building. In these cases wind enters the windward opening and leaves the building through both the leeward side and the window. It is quite clear that with the increment of the approaching wind angle, the pressure reduces at the entrance aperture. This decrement of the

pressure goes on until the wind angle reaches about 50° where the pressure at the entrance opening reaches the pressure at the window place. Pressure drops in the direction of the airflow cause it not to leave the building through the window and hence the whole flow goes out through the leeward opening. With a slight increase in the wind angle, the pressure of the window and the entrance opening will be close to each other more and more. This process will allow the air to enter from the window to the inside part of the building. In this stage the airflow pattern will experience its second region and the windward opening and the window will act as supply segments. This region is extended between wind angles of 50° and 65°. This flow pattern will continue until the transition angle of the windward side. Transition angle is defined as the angle at which there is no air flow through the windward side of a wind catcher [5]. Finally in the third flow pattern, the pressure at the window becomes greater than the ones at both the windward and leeward openings. In such a situation, wind enters the window part and leaves through these two apertures. It shows that the CFD results are in relatively satisfactory agreement with the experimental data. There is a difference between these results near the transition angle of the windward segment [60-75°]. This difference can be evaluated by determining the accuracy of measured experimental data.

CFD can help to assess the accuracy of measurement procedures and the uncertainty of experimental results. In this study, several pitot and static tubes were used in order to determine the induced air flow rate into the test room. As it has been mentioned in the section 2.2.2, these square-ended probes which were placed at the bottom of the windward and at the top of the leeward segments and parallel to the channel axis begin to show error near 18° flow inclination. Figure 9 shows the distribution of the velocity vector angles with respect to channel axis (z axis). It is clear that less values of this angle indicate more alignment of the velocity vectors with the channel axis and the axis of the pitot and static tubes. As it is obvious in this figure, there is some errors in measured experimental data due to directional sensitivity of the probes at the wind direction of 60°, which is the main reason for difference between experimental and CFD results in this angle.

In the present study, it was assumed that there is no short-circuiting and air flow through the window can be obtained using the algebraic sum of these two values. Figure 10 shows the path lines of the particles that are released from a virtual surface vertical to the wind catcher opening. It can be seen that for lower values of air incident angle air enters the building with no short-circuiting. With increasing the air incident angle, the short-circuiting appears into the wind catcher system and reaches to its maximum value at 60°.

Figure 11 shows the simulation results of the wind velocity distribution around the wind catcher for different air incident angles. This figure also shows the path lines of the particles which are released from a virtual line parallel to the wind catcher opening. Smoke visualization tests were carried out to demonstrate the top view of the passing flow through the wind catcher for various wind angles. The results are also shown in this figure. As it is shown in Fig. 11, placing the wind catcher on the route of prevailing wind streams (zero angle), will cause the maximum entrance flow rate into the windward segment. With increasing the air incident angle the vortices which appear into the channel and perpendicular to the air passage, decrease the induced air flow rate. Also with increasing the wind angle and hence developing the region of influences of vortices, the induced operation of wind catcher will reduce continuously to its minimum value at the ‘‘transition angle’’ [5]. Exceeding the wind angle over the transition angle, will cause a change in air flow direction into the windward side. In this situation, windward and leeward segments act as suction devices. This is due to the fact that exposing the body of the wind catcher on the route of air stream causes a low pressure wake region behind it and posing its openings there in that region with a pressure lower than the environment pressure, will result in an air flow from window to the wind catcher openings.

Figure 12 shows average pressure coefficients at the upper part of the windward and leeward segments for different values of approaching air incident angles. Because of exposing to the air stream, Cp experiences its maximum value at zero air incident angle for the windward side. By increasing the wind angle, average pressure coefficient drops rapidly to reach its minimum value at 90°. For the leeward side of the wind catcher, almost uniform pressure distribution is observed. This is because of that after the separation of the air stream from the side surfaces an almost uniform low-pressure wake is formed around the back face. The largest negative pressure on the leeward side of the model occurs at 90° wind angle. It should be mentioned that similar trends have been reported by other researchers [2, 5]. The inside pressure coefficient estimated by analytic model is also presented in this figure. It can be seen that by increasing the wind angle, the inside pressure drops and reaches its minimum value at 90°. It should be noted that because of exposing the window of the house to the atmospheric environment, the pressure coefficient of this segment will be constant for all air incident angles.

In Fig. 13, the air flow rate obtained from the CFD simulation and analytic method has been compared with the experimental results. It can be seen that CFD simulation and analytic model results have a good agreement with the experimental results though there are some differences at the leeward segment as well as near the transition angle of the windward side.

The comparison factor can be used to compare the performance of different wind catchers. The comparison factor of a two-sided wind catcher against the one-sided one versus air incident angles is shown in Fig. 14. It is seen that, in the first flow pattern, the comparison factor is nearly equal to 2. This means that in the area where

there is prevailing wind, from economic and designing viewpoints, the one-sided wind catcher is more suitable. By increasing the wind angle and hence domination of the second flow pattern, the comparison factor decreases. This drop continues until its minimum value at the transition angle. In this angle, there is no flow rate through the one-sided wind catcher and its house; therefore, the value of comparison factor is equal to zero. Exceeding the wind angle over the transition angle of the windward side will cause an increase in comparison factor. For these wind angles, a local maximum occurs at the transition angle of the leeward side of the two-sided wind catcher.

The most important advantage of a two-sided wind catcher is related to the angle in which the one-sided wind catcher exposes under the transition angle and the airflow rate through it tends to zero. In other words, in the area where there is prevailing wind, from economic and designing viewpoints, the one-sided wind catcher is more suitable.

5. Conclusions

Experimental wind tunnel and smoke visualization testing as well as CFD and analytical modeling were conducted to investigate the performance of a two-sided wind catcher. The two-sided wind catcher model was constructed from two similar one-sided wind catcher models, which were attached together back to back. These one-sided models are 1: 40 scale models of Kharmani's School wind catcher in Yazd. The wind catcher model was connected to a house model, which was erected beneath the wind tunnel. The house model had a vertical openable window that was placed at the back of it. The induced volumetric airflow and the pressure coefficients around all surfaces of the wind catcher model were measured at various air incident angles. Furthermore, the CFD commercial code was also used to evaluate the pressure coefficient distributions and airflow pattern around and through the wind catcher. Additional experimental tests and CFD simulation in the wind catcher were also conducted in order to assess the accuracy of measurement procedures and the uncertainty of experimental results. Also using measured pressure coefficients the theoretical values of ventilated air flow were estimated to evaluate ability of simplified models in natural ventilation studies.

The natural ventilation performance of wind catchers strongly depends on the pressure coefficients at the wind catcher openings. These coefficients vary sharply with the air incident angle. Because of exposing to the air stream, Cp experiences its maximum value at zero air incident angle at the windward side. By increasing the wind angle, average pressure coefficient drops rapidly to reach its minimum value at 90°. For the leeward side of the wind catcher, almost uniform pressure distribution is observed. The inside pressure coefficient can be estimated by an analytic model. It can be seen that by increasing the wind angle, the inside pressure drops and reaches its minimum value at 90°.

CFD simulation and analytic model results have a good agreement with the experimental results though there are some differences at the leeward segment as well as near the transition angle of the windward side. CFD predictions represent ideal conditions for the testing. At the transition angle there is some errors in measured experimental data due to directional sensitivity of the probes which is the main reason for differences between experimental and CFD results in this angle. However, all these tools provide an interesting tool for modeling of wind catchers natural ventilation systems.

Short-circuiting is a harmful phenomenon in wind catcher systems which causes the air enters through supply openings and leaves through another without flowing inside the house. For a two-sided wind catcher and for lower values of air incident angle air enters the building with no short-circuiting. With increasing the air incident angle, the short-circuiting appears into the wind catcher system and reaches to its maximum value at 60°.

The most important advantage of a two-sided wind catcher is related to the angle in which the one-sided wind catcher opening exposes under the transition angle and the airflow rate through it tends to zero.

Acknowledgement

The authors would like to thank the thermodynamics laboratory of the school of Mechanical Engineering of Yazd University for providing the test rig and experimental facilities.

References

[1] Fathy H. Natural energy and vernacular architecture: principles and examples with reference to hot arid climates. Chicago, IL: The University of Chicago Press; 1986.
[2] Karakatsanis C, Bahadori MN, Vickery BJ. Evaluation of pressure coefficients and estimation of air flow rates in buildings employing wind towers. Solar Energy 1986; 37(5):363–374.
[3] G.S. Battle, M. Zanchetta, P. Heath, Wind towers and wind driven ventilation, in: A. Sayigh (Ed.), World Renewable Energy Congress VI (WREC2000), Elsevier Science Ltd., Brighton, 2000, pp. 432–437.

[4] Nouane´gue´ H.F., Alandji L.R., Bilgen E., Numerical study of solar-wind tower systems for ventilation of dwellings. Renewable Energy 2008; 33(3): 434-443
[5] Montazeri, H. and Azizian, R. Experimental study on natural ventilation performance of one-sided wind catcher. Building and Environment 2008; 43(12): 2193–2202.
[6] M. N. Bahadori, Passive cooling systems in Iranian architecture, Scientific American 1978; 238 (2): 144-154.
[7] Elmualim AA, Awbi HB. Wind tunnel and CFD investigation of the performance of wind catcher ventilation systems. International Journal of Ventilation 2002; 1(1):53–64.
[8] Liu L, Mak CM. The assessment of the performance of a wind catcher system using computational fluid dynamics. Building and Environment 2007; 42(3):1135–1141.
[9] Elmualim AA. Effect of damper and heat source on wind catcher natural ventilation performance. Energy and Buildings 2005; 38(8):939–948.
[10] Hughes BR, Ghani SAA. A numerical investigation into the effect of windvent dampers on operating conditions. Building and Environment 2009; 44(2): 237–248
[11] Etheridge D., Sandberg M. Building ventilation: Theory and Measurement. UK: Wiley; 1996.
[12] Etheridge D. Natural ventilation through large openings - measurements at model scale and envelope flow theory. International Journal of Ventilation 2004; 2(4): 325-342
[13] Bahadori M, Haghighat F. Passive cooling in hot arid regions in developing countries by employing domed roofs and reducing the temperature of internal spaces. Building and Environment 1985; 20(2):103–113.
[14] Jones M., Kirby R. Quantifying the performance of a top-down natural ventilation Windcatcher™. Building and Environment 2009; 44(2):1925–1934.
[15] Bauman FS, Ernest DR, Arens EA. The effects of surrounding buildings on wind pressure distributions and natural ventilation in long building rows. ASHRAE Transactions 1988; 94 (Part 2):1670–1696.
[16] Asfour O. S., Gadi M. B. A comparison between CFD and Network models for predicting wind-driven ventilation in buildings. Building and Environment 2007; 42(12): 4079–4085
[17] Tropea, C.,Yarin, A. L., and Foss J. F. Springer handbook of experimental fluid mechanics, 2007 (Springer-Verlag, Berlin, Heidelberg).
[18] Dudziniski, T. J. and Krause, L. N. Effect of inlet geometry on flow-angle characteristics of miniature total-pressure tubes. NACA TN D-6406, 1971.

FIGURES

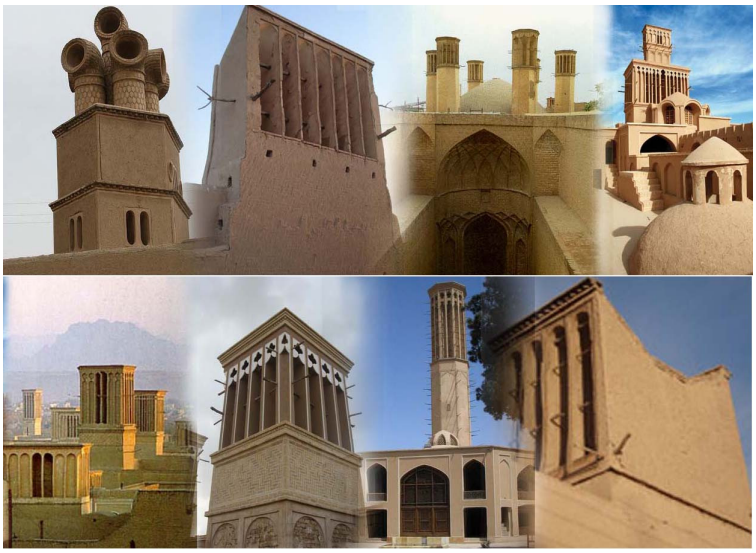

Fig. 1. Several ancient wind catchers with different configurations in the city of Yazd

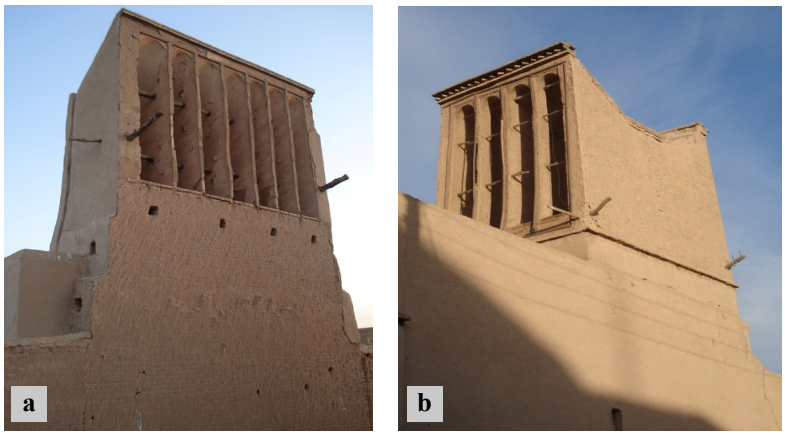

Fig. 2. (a) Kharmani's School Baud-Geer, (b) an ancient two-sided wind catcher.

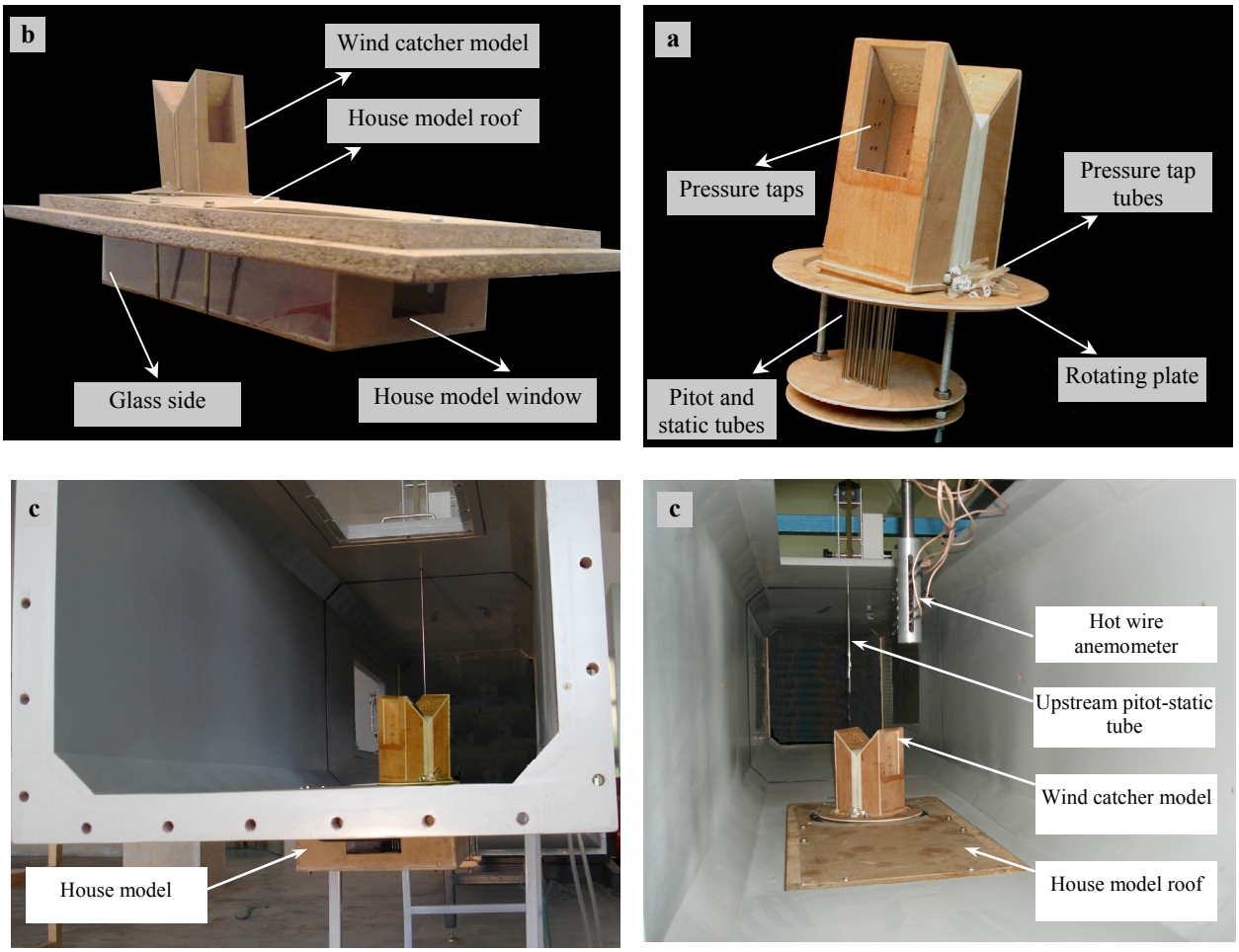

Fig. 3. (a) Two-sided wind catcher model with the attached pressure tabs, pitot and static tubes, (b) the house model along with the wind catcher model, (c) the wind tunnel and experimental test rig.

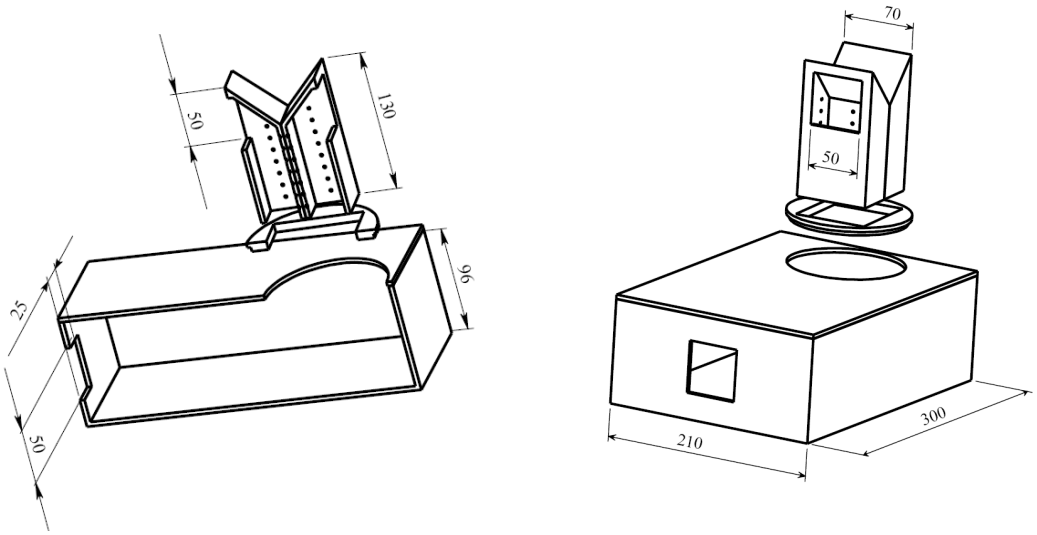

Fig. 4. Isometric view of two-sided wind catcher model and its connected house model along with their dimensions and locations of pressure taps. All dimensions are in millimeter.

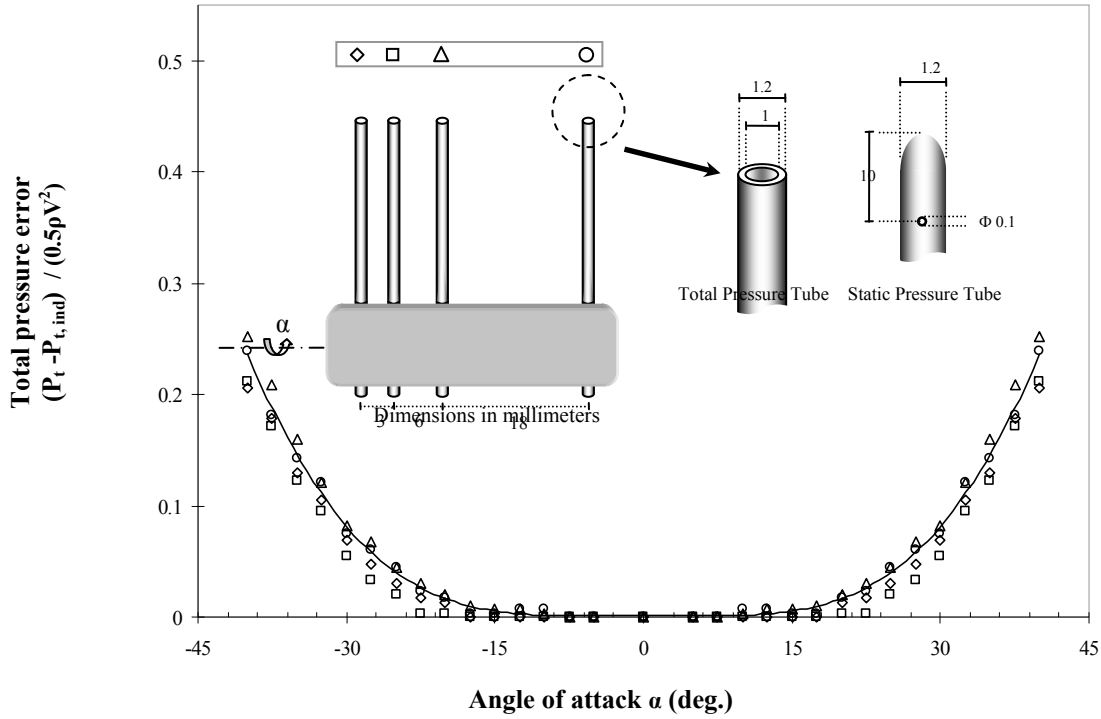

Fig. 5. Yaw sensitivity of four pitot probes used in the present study.

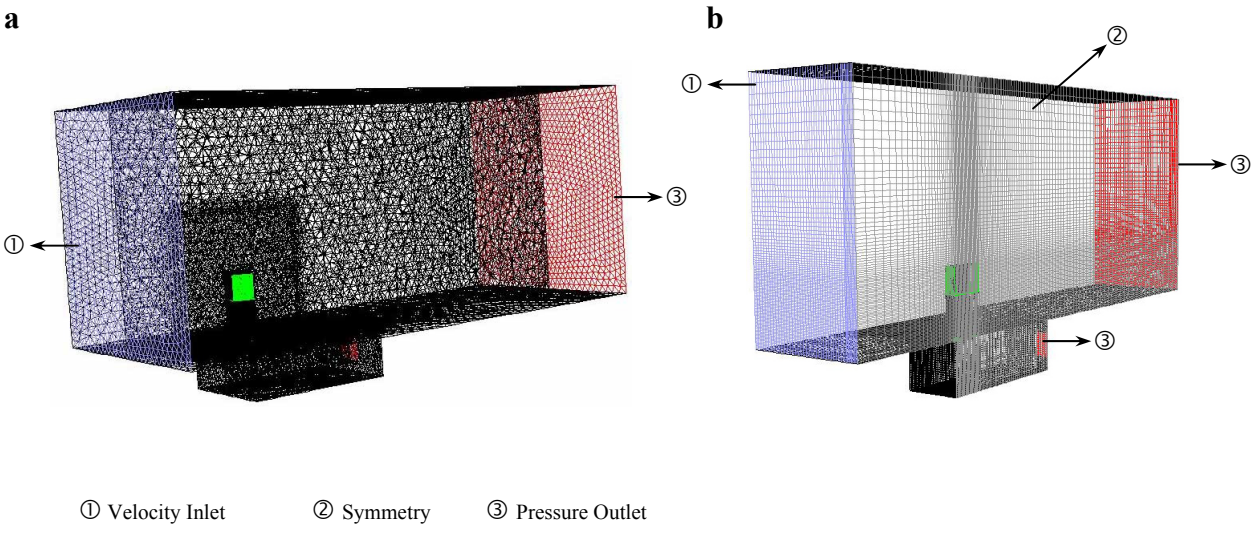

Fig. 6. Meshing of the simulated wind tunnel, wind catcher and test room along with boundary conditions (a) unstructured grid (15°- 75°) (b) structured grid (0° and 90°).

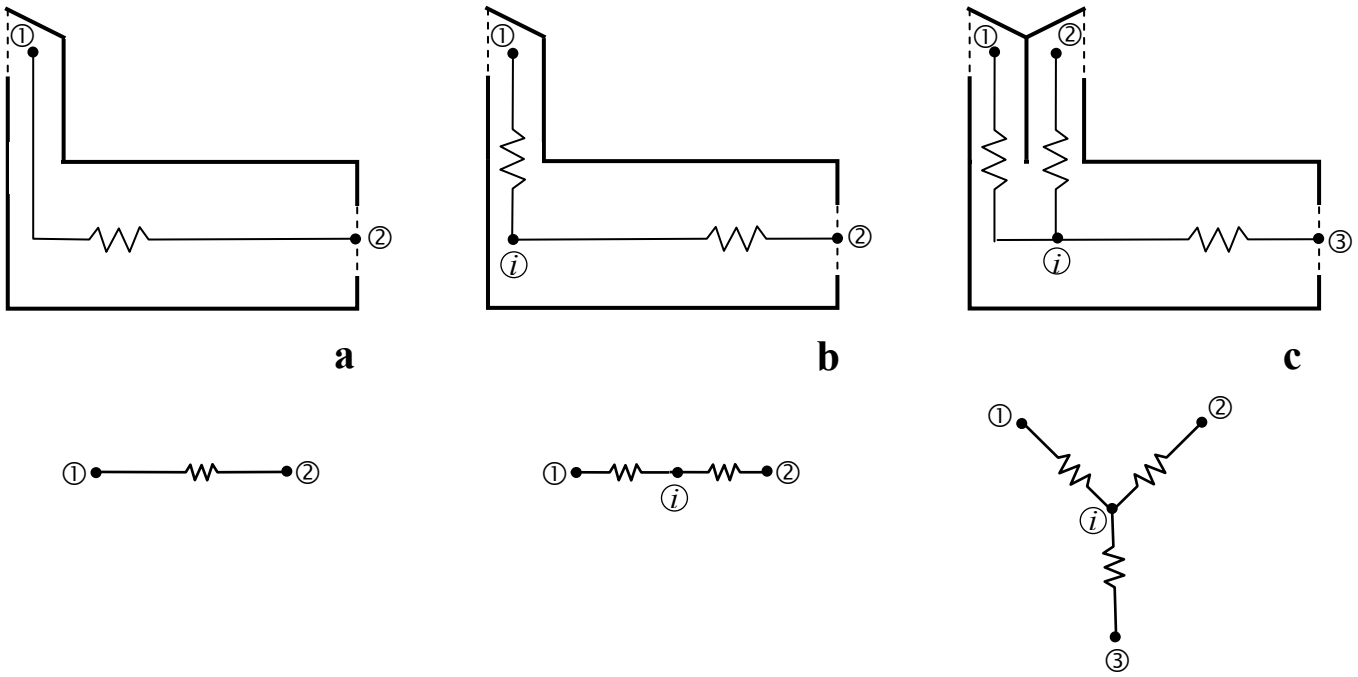

Fig. 7. A flow network representing ventilation through a room (a, b) with a one-sided wind catcher (c) with a two-sided wind catcher.

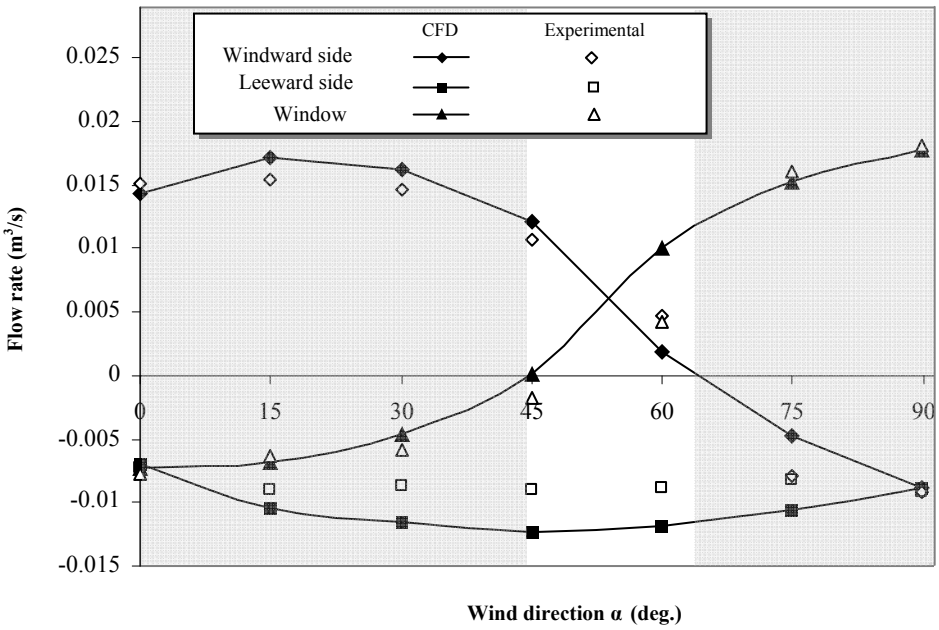

Fig. 8. Measured volumetric airflow through the windward and leeward sides and through the window of the house.

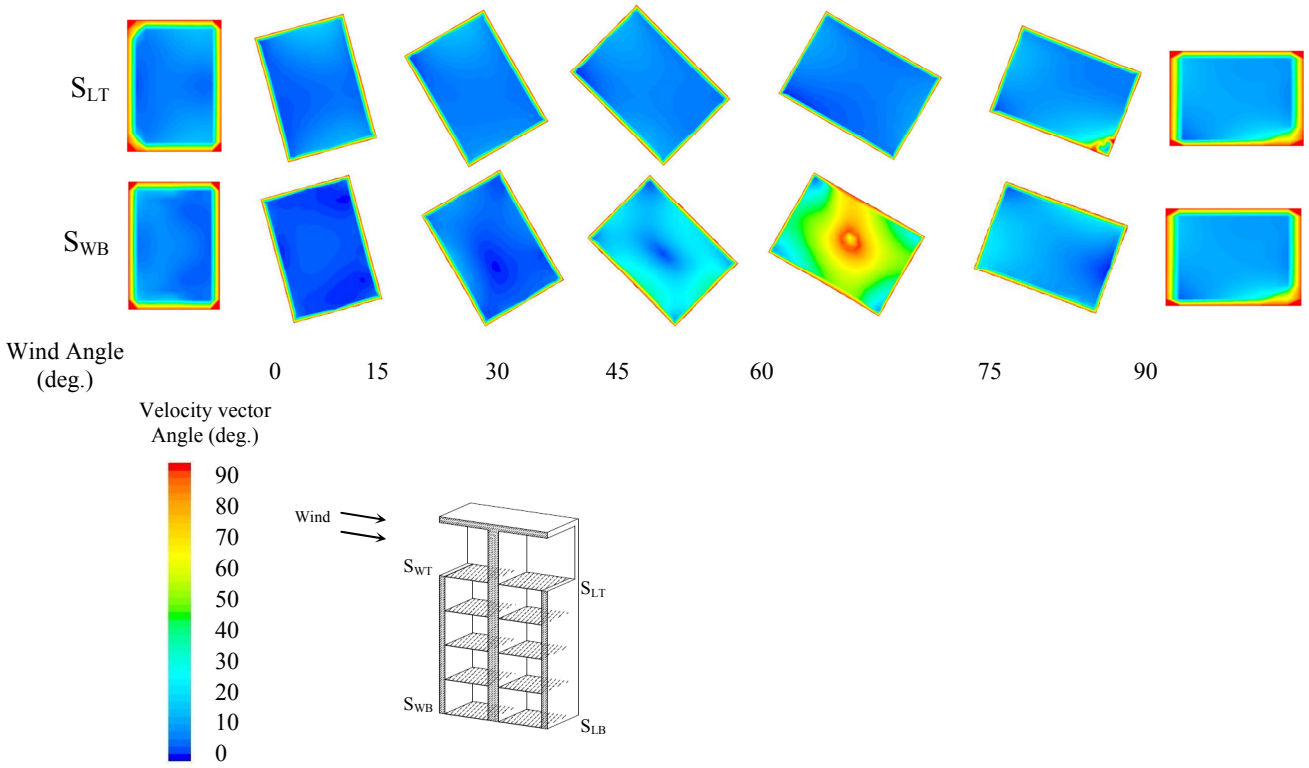

Fig. 9. Distribution of the velocity vector angles with respect to channel axis at the bottom of the windward and at the top of the leeward segments.

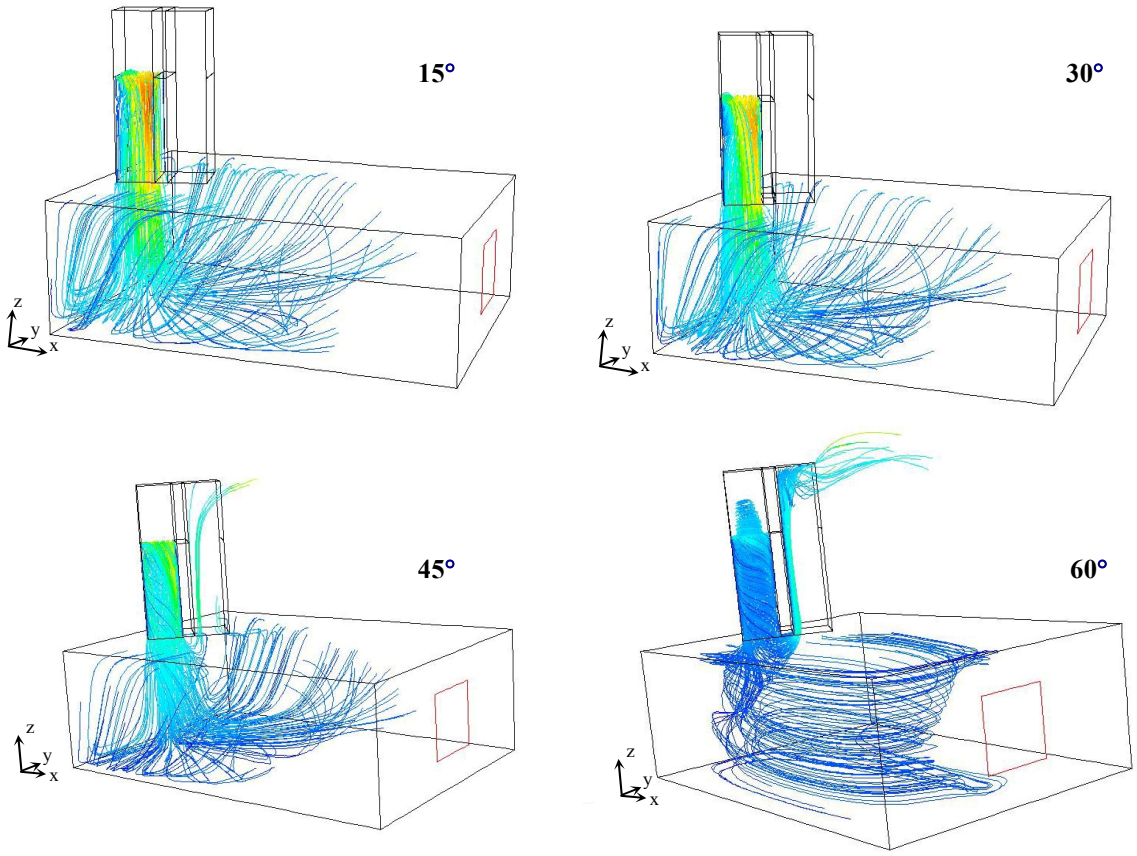

Fig. **10.** Path lines of the particles that are released from a virtual surface vertical to the wind catcher opening.

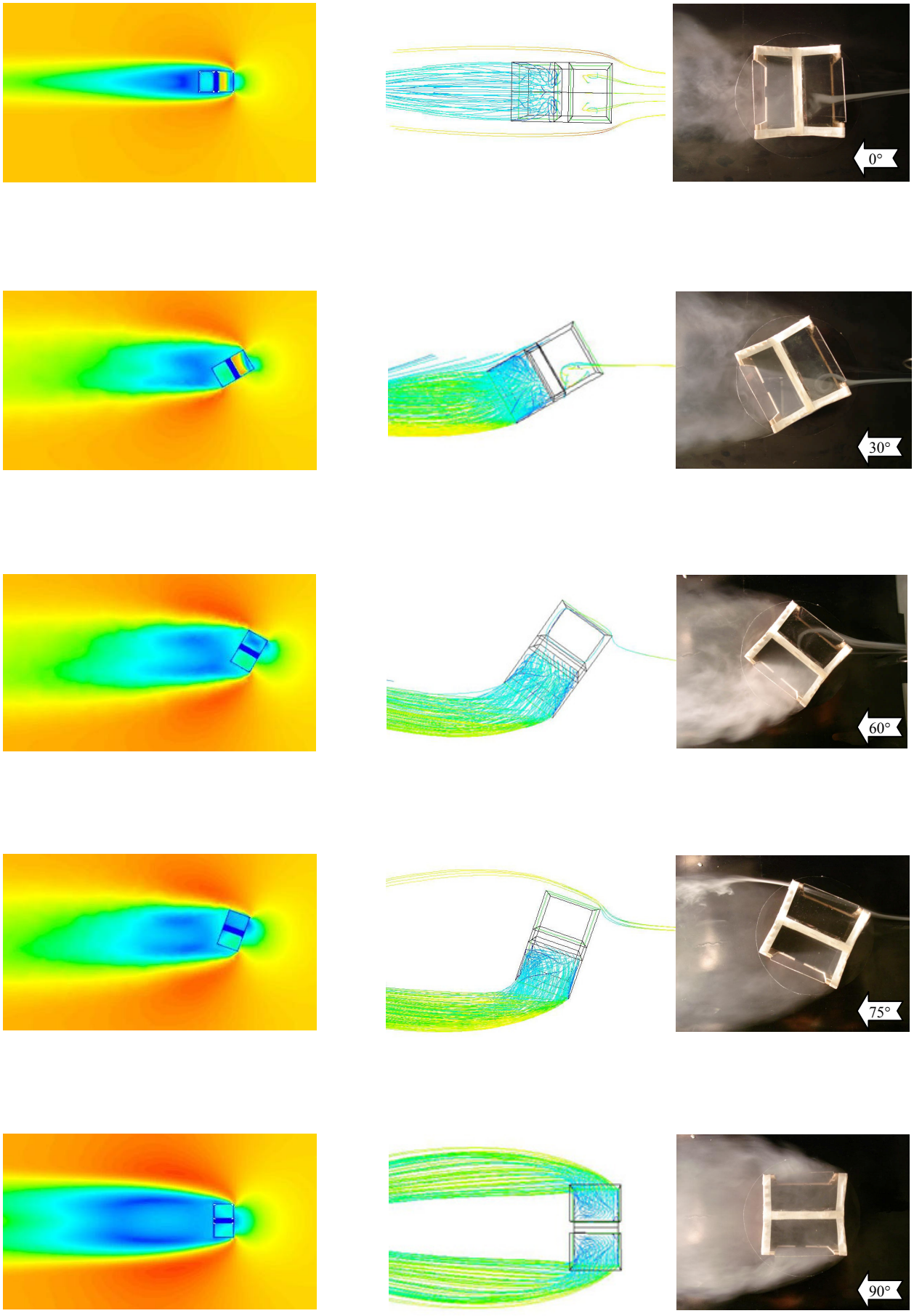

Fig. 11. Top view of the passing flow around the wind catcher for different wind angles.

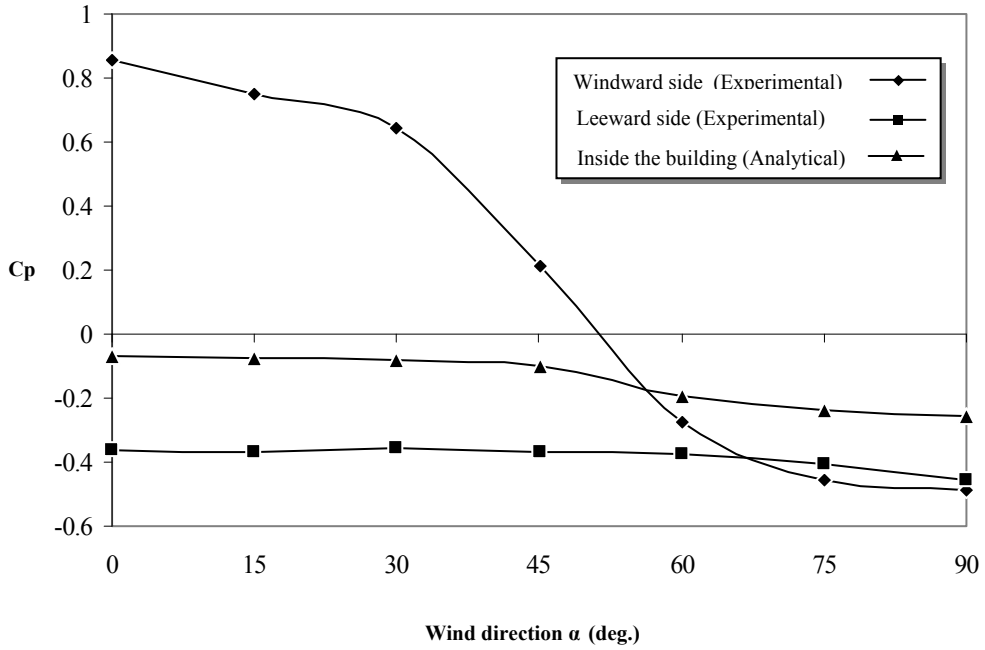

Fig. 12. Average pressure coefficients at the upper parts of the windward and leeward segments and predicted pressure coefficient inside the building.

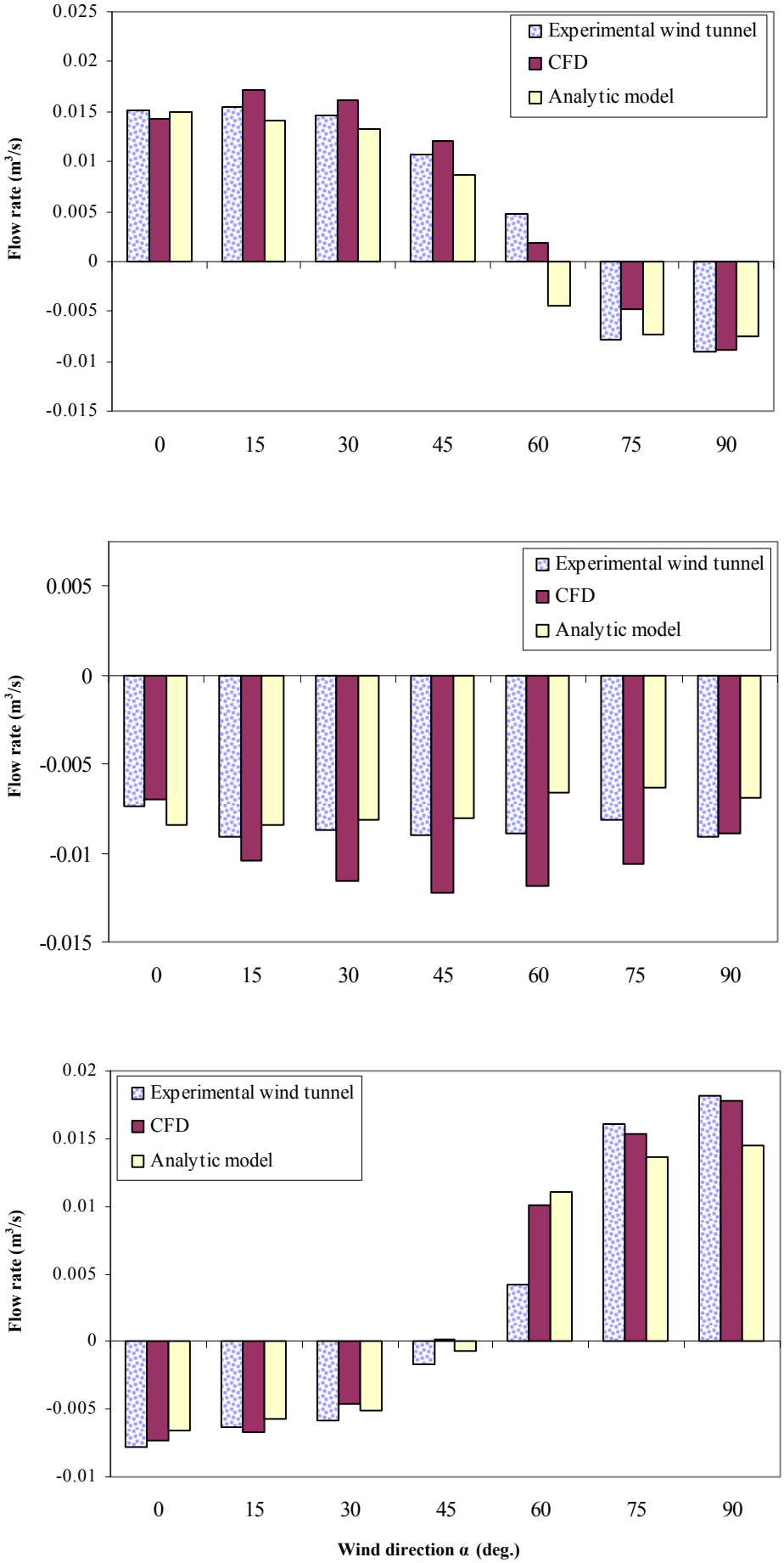

Fig. 13. Comparison of the simulation and experimental results: (a) windward side (b) leeward side (c) window.

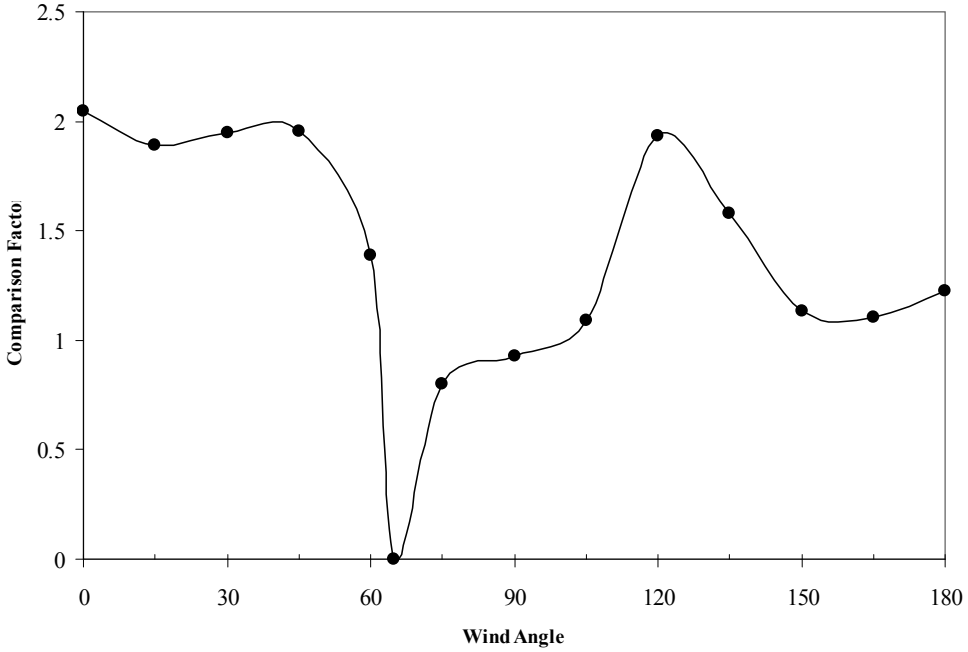

Fig. 14. The comparison factor of a two-sided wind catcher against the one-sided one [6] versus air incident angles.

TABLES

Table 1. Summary of CFD analysis.

Program	CFD		FLUENT 6.3.26
	Grid Generation		Gambit 2.0
Discretization scheme	Second Order		
Algorithm	Steady state (SIMPLE)		
Boundary Condition	Inlet		Velocity : 20 m/s
	Outlet	Wind tunnel outlet	Gage pressure : 0 [pa]
		Window	
	walls		Wall : no slip Symmetry: free slip (0° and 90°)
The number of grids	492080 - hexahedral (0° and 90°) 1200000 – tetrahedral (15° - 75°)		
Turbulence model	Reynolds Stress Model K-ε (0° and 90°) RNG K- ε (0° and 90°)		

Table 2. Pressure coefficients and airflow rate values used in analytical model along with predicted discharge values.

α	One-sided [5]				Two-sided				
	C_p	Q (m^3/s)		C_{dt}	C_p		Q (m^3/s)		
	Opening	Opening	Window		Windward	Leeward	Windward	Leeward	Window
0	0.81	0.0155	-0.0155	0.42	0.85	-0.36	0.0152	-0.0073	-0.0078
15	0.81	0.0146	-0.0146	0.39	0.75	-0.37	0.0154	-0.0091	-0.0064
30	0.71	0.0142	-0.0142	0.41	0.64	-0.36	0.0146	-0.0087	-0.0059
45	0.38	0.0105	-0.0105	0.39	0.21	-0.37	0.0108	-0.0090	-0.0017
60	0.08	0.0062	-0.0062	0.38	-0.28	-0.37	0.0047	-0.0089	0.0042
75	-0.16	-0.0064	0.0064	0.66	-0.46	-0.40	-0.0079	-0.0082	0.0161
90	-0.30	-0.0085	0.0085	0.49	-0.49	-0.46	-0.0091	-0.0091	0.0182
105	-0.33	-0.0087	0.0087	0.47	-0.40	-0.46	-0.0082	-0.0079	0.0161
120	-0.36	-0.0086	0.0086	0.43	-0.37	-0.28	-0.0089	0.0047	0.0042
135	-0.38	-0.0085	0.0085	0.41	-0.37	0.21	-0.0090	0.0108	-0.0017
150	-0.39	-0.0083	0.0083	0.39	-0.36	0.64	-0.0087	0.0146	-0.0059
165	-0.40	-0.0085	0.0085	0.40	-0.37	0.75	-0.0091	0.0154	-0.0064
180	-0.43	-0.0093	0.0093	0.42	-0.36	0.85	-0.0073	0.0152	-0.0078
					$C_{d,leeward}=C_{d,windward}=0.4$			$C_{d,window}=0.75$	

Table 3. Measured airflow through the wind catcher system for various predicted models.

case		Wind direction					
		0°			90°		
		windward	Leeward	Window	windward	Leeward	Window
Experimental wind tunnel		0.0152	0.0073	0.0078	0.0091	0.0091	0.0182
CFD	RSM	0.0143	0.0070	0.0073	0.0089	0.0089	0.0177
	k-ε	0.0163	0.0075	0.0091	0.0092	0.0092	0.0183
	RNG *k*-ε	0.0148	0.0077	0.0071	0.0090	0.0090	0.0180